Cr(III) removal from aqueous solutions: A straightforward model approaching of the adsorption in a fixed-bed column

ANTONIO DAVID DORADO[1], XAVIER GAMISANS[1]*, CESAR VALDERRAMA[2], MONTSE SOLÉ[1] and CONXITA LAO[1]

[1] *Department of Mining Engineering and Natural Resources. Universitat Politécnica de Catalunya, Escola Politécnica Superior d'Enginyeria de Manresa, Manresa, Spain.*

[2] *Department of Chemical Engineering. Universitat Politécnica de Catalunya, Escola Técnica Superior d'Enginyeria Industrial de Barcelona, Barcelona, Spain.*

_____

*Address correspondence to Dr. Ing. Xavier Gamisans EPSEM, Universitat Politécnica de Catalunya (UPC). Bases de Manresa, 61-73, 08242-Manresa, Spain;
Tel.: +34938777234, Fax.: +34938777202.
E-mail: xavierg@emrn.upc.edu

Abstract

Prediction of breakthrough curves for continuous sorption characterization is generally performed by means of simple and simplified equations. These expressions hardly have any physical meaning and, besides, do not allow extrapolation. A novel and simple approach, based on unsteady state mass balances, is presented herein for the simulation of the adsorption of Cr(III) ions from aqueous onto a low-cost adsorbent (leonardite). The proposed model overcomes the limitations of the commonly used analytical solution-based models without the need for complex mathematical methods. A set of experimental breakthrough curves obtained from lab-scale fixed-bed columns was used to calibrate and validate the proposed model with a minimum number of parameters to be adjusted.

Keywords: Adsorption, chromium, continuous, breakthrough curve, modeling

Introduction

Chromium is usually found in some industrial sewage such as electroplating, leather, tanning and textile industries. Chromium mostly exists in two states, Cr(III) and Cr(VI). Cr(VI) has been classified as a Group I human carcinogen by the International Agency for Research on Cancer (IARC) and as a Group A inhalation carcinogen by the US Environmental Protection Agency (USEPA). Hexavalent chromium is 500 times more toxic than the trivalent form. Moreover, Cr(III) may be readily oxidized to Cr(VI) by certain circumstances of pH changes and redox potential conditions.[1] Consequently, the removal of chromium from industrial wastewaters is a research topic of great

interest. Several procedures have been proposed to remove chromium from industrial wastewater. [2-5] These methods include different chemical procedures based on reduction and precipitation processes or even ion exchange processes. Although the effectiveness of these procedures has been sufficiently proved, they present some inconveniences and limitations. These are mainly two, the high volume of aqueous solution of colloidal chromium hydroxide handled and their relatively high cost. Recently, chromium adsorption onto low-cost sorbents has been investigated as an alternative for current costly methods. Among these materials, immature coals (such as leonardite) have already demonstrated their ability to efficiently adsorb pollutants of different nature. [6-8]

Most studies related to adsorption of chromium are performed in batch mode. [9] Batch adsorption tests give fundamental information for a particular sorbent-sorbate pair in terms of sorption capacities and kinetics. However, in the majority of practical (industrial) applications, batch systems are scarcely found. Continuous operation is the most suitable mode from both an economical and process control point of view.

The continuous sorption process is usually characterized by the so called breakthrough curves, i.e. a representation of the pollutant effluent concentration versus time profile in a fixed bed column. In addition, breakthrough curves prediction through mathematical models is a useful tool for scale-up and design purposes. Mechanistic models for fixed-bed adsorption columns should include different phenomena such as: axial dispersion, film diffusion resistance, intra-particle diffusion resistance (both pore and surface diffusion) and sorption equilibrium with the sorbent. The inclusion of all these processes involves rigorous but mathematically complex models associated with non-linear partial differential equations. This implies using numerical solutions and, thus, a time-consuming process framework. In addition, the use of comprehensive mechanistic

models involves the adjustment of several parameters, i.e. the availability of several sets of reliable and well-designed experimental data is required. For this reason, in the last decades a wide variety of semi-empirical models have been stated in order to predict the behavior of the fixed-bed adsorption process through the simulation of the breakthrough curves response.

From the above mentioned, the aim of this study is to compare the most commonly used analytical models for the breakthrough curves characterization for heavy metals adsorption in fixed bed columns. Besides, a new approach based on rigorous mass balances and using the minimum number of adjusted parameters is proposed. The new model approach is developed, calibrated and validated for the adsorption of Cr(III) from synthetic solutions by a fixed bed column packed with leonardite.

Materials and Methods

Materials

The leonardite used as adsorbent in this study was supplied by Sociedad Española de Acidos Húmicos, S.A. (SEPHU®, Zaragoza, Spain). This adsorbent was sieved to a grain size of 0.09–0.2 mm before its use in the sorption experiments. Some of its physical and chemical characteristics are shown in Table 1.

Chromium stock solution was prepared by dissolving a known quantity of $Cr(NO_3)_3 \cdot 9H_2O$ (AR grade) in Milli-Q® water. The stock solution was then diluted to obtain standard solutions. All chemicals were of analytical reagent grade (Scharlau®). The amount of Cr(III) in the solutions before and after the adsorption tests was determined by flame atomic adsorption spectrophotometry (FAAS), using a Termo Electron Corporation (SOLAAR S2 model) spectrophotometer with an acetylene-

nitrous oxide flame. The wavelength was 359 nm. All experiments were performed twice. The repeatability of the results showed a variation coefficient of less than 5%.

Continuous Experiments

Fixed-bed column studies were conducted using laboratory-scale polyethylene columns of 1 cm diameter and 70 mm length. The columns were packed with known quantities of Leonardite to obtain a particular bed depth. A glass wood plug was placed at the bottom to support the adsorbent bed as well as to prevent the absorbent washing out. Another plug was also placed on top of the bed to prevent floating up of the leonardite. To ensure complete purge of the trapped air, leonardite packed columns were fully wetted by filling them with deionized water for 5 h prior starting the experiments. The influent Cr(III) was supplied and maintained in each column throughout the experiments by using a peristaltic pump (ISMATEC mod. MPC). The flow rate was cross-checked at the exit of the column at regular intervals of 200 min to prevent and minimize any flow fluctuations (if occurred) inside the column bed.

Breakthrough curve determination experiments were carried out in 6 different columns. The same flow-rate (0.33 cm^3 min^{-1}), amount of adsorbent (2 g) and solution volume (1 L) were applied in each column. The chromium (III) concentration varied from 20 to 150 mg L^{-1}. Effluent samples were collected with an automated sampler every 200 minutes from 0 to 3000 min. Chromium content in each sample was analyzed as described above.

Analytical mathematical approaches

a) Bed Depth Service Time (BDST) (Bohart-Adams model)

Even though Borhart and Adams [10] equation was originally developed for gas-solid systems, it has been widely used in the literature for liquid-solid systems. [11, 12] The BDST model describes the relationship between the bed depth and the column service time according to the following equation:

$$ln\left(\frac{C_0}{C}-1\right)=ln\left[exp\left(kN_0\frac{Z}{U}\right)-1\right]-kC_0t \quad (1)$$

Where C_0 is the initial sorbate concentration (mg L^{-1}), C is the sorbate concentration at time t (mg L^{-1}), k is the sorption rate constant for the column (L min^{-1} mg^{-1}), Z is the length of the column bed (m), N_0 is the sorptive capacity of the sorbent (mg L^{-1}) and U is the linear flow velocity of the liquid phase (m min^{-1}).

This expression can be rearranged to:

$$\frac{C}{C_0}=\frac{exp(kC_0t)}{exp\left(kN_0\frac{Z}{U}\right)-1+exp(kC_0t)} \quad (2)$$

b) Thomas model

The Thomas [13] model considers plug-flow behavior in the bed, coupled to Langmuir isotherm for equilibrium and second-order reversible reaction kinetics. The most usual expression for Thomas model is:

$$\frac{C}{C_0}=\frac{1}{1+exp[k_T(q_0m_C-C_0V_{eff})/Q]} \quad (3)$$

Where K_T is the Thomas model constant (L min^{-1} mg^{-1}), q_0 is the maximum solid-phase concentration of the solute (mg g^{-1}), m_C is the mass of sorbent in the column (mg), V_{eff} is the throughput volume (L) and Q is the volumetric flow rate (L min^{-1}).

c) Yoon and Nelson model

Similarly to the BDST model, the Yoon and Nelson [14] model was originally developed for the adsorption of gaseous sorbates in activated carbons by means of a simple equation:

$$ln\left(\frac{C}{C_0-C}\right) = k_{YN}t - t_{0.5}k_{YN} \quad (4)$$

Where K_{YN} is the Yoon-Nelson rate constant (min^{-1}) and $t_{0.5}$ is the time required for 50% sorbate breakthrough (min). This expression can be rearranged to:

$$\frac{C}{C_0} = \frac{1}{1+exp[k_{YN}(t_{0.5}-t)]} \quad (5)$$

d) Clark model

Clark [15] model was derived from a mass balance on a differential element in a fixed bed coupled with Freundlich isotherm for the liquid-solid equilibrium. One possible expression of the model is the following:

$$\frac{C}{C_0} = \left(\frac{1}{1+Aexp^{-rt}}\right)^{1/n-1} \quad (6)$$

Where n is the Freundlich constant (-) and A (-) and r (min^{-1}) are Clark's model parameters.

166

167 *e) Wolborska model*

168 Wolborska [16] deduced an equation from mass balances in a column considering
169 external mass transfer and constant kinetic coefficients. The final form of the equation is
170 the following:

171

172 $$ln\frac{C}{C_0} = \frac{\beta C_0}{N_0}t - \frac{\beta Z}{U} \quad (7)$$

173

174 Where β is the kinetic coefficient of external mass transfer (min^{-1}).

175

176 *f) Dose-Response model*

177 The Dose-Response model [17] is based on mathematical issues instead of mechanistic
178 fundamentals. However its final form is similar to Thomas and Yoon-Nelson models.

179

180 $$\frac{C}{C_0} = 1 - \frac{1}{1+(C_0 V_{eff}/q_o m_C)^a} \quad (8)$$

181

182 Where a is the Dose-Response model parameter (-).

183

184 ***New modeling approach***

185 The new modeling approach is based on the well-known diffusion-reaction
186 mathematical model which has been successfully used in a wide range of chemical
187 engineering related systems [18].

188 The unsteady state model proposed is based on the following assumptions:

189 1. Isothermal conditions across the column and along the time.

2. The aqueous phase circulation regime is modeled as a plug flow pattern. Thus, axial dispersion is not considered.

3. Planar geometry and perpendicular diffusion in the adsorbent is used to derive the model equations.

4. The aqueous-solid interface resistance is negligible.

5. The Aqueous-solid interface equilibrium is described by Langmuir's isotherm.

6. An effective interfacial area exists, thus considering the possibility of dry zones.

7. There is a maximum penetration depth for the pollutant into the solid phase.

These assumptions can be easily justified by means of the experimental conditions and the column dimensions. The Langmuir isotherm equilibrium behavior was derived from previous batch experiments. [19]

Considering the above listed assumptions, the following mass balance for the liquid phase can be stated:

$$\frac{\partial C}{\partial t} = -\frac{Q}{a_c \cdot \varepsilon}\frac{\partial C}{\partial z} - \frac{D \cdot a_s}{\varepsilon}\left(\frac{\partial N_0}{\partial x}\right)\Bigg|_{x=0} \qquad (9)$$

With the following boundary condition: at z=0, C = C0.

Where C is the Cr(III) liquid concentration (mg L^{-1}), Q is the volumetric liquid flowrate (L min^{-1}), a_c is the cross-sectional area of the column (dm^2), ε is the packed bed porosity, z is the height position across the column (dm), D is the effective diffusion coefficient of the solute (dm^2 min^{-1}), a_s is the effective sorbent material specific area (m^2 dm^{-3}), N_0 is the sorptive capacity of the sorbent (mg dm^{-3}), x is the depth from the sorbent material surface (dm) and C_0 is the column inlet Cr(III) concentration (mg L^{-1}).

Regarding to the solid phase, the following mass balance was formulated:

$$\frac{\partial N_0}{\partial t} = D\frac{\partial^2 N_0}{\partial x^2} \qquad (10)$$

This equation accounts for the time-dependent variation of the solid phase concentration due to diffusion fluxes. This equation needs the following boundary conditions (including the Langmuir isotherm expression) to be solved:

$$\text{at } x = 0,\ N_0 = \rho \frac{q_0 \cdot q_1 \cdot C}{1 + q_1 \cdot C} \text{ and at } x = \delta,\ \frac{\partial N_0}{\partial x} = 0 \qquad (11)$$

Where ρ is the sorbent density (mg dm^{-3}), q_0 is the maximum solid-phase concentration of the solute (75.2 mg g^{-1}), q_1 is the Langmuir isotherm parameter (0.061 dm^3 mg^{-1}) and δ is maximum penetration depth for the pollutant into the solid phase (dm).

Models' Solution

Analytical models

Nonlinear regressions were performed by MATLAB software to fit the experimental data to the six different models. Non-linear regression avoids the bias error that might appear from using different linearization procedures. MATLAB package uses nonlinear least-squares data fitting by the Gauss-Newton method, which converged quickly and gave better results than other commercial software (e.g. EXCEL™ Solver).

Numerical approach

The set of partial differential equations was discretized in space along the bed height and sorbent thickness. The resulting set of ordinary differential equations was solved using MATLAB in a home-made modeling environment. A variable order method was used for solving stiff differential equations based on the numerical differentiation formulas (NDFs). The maximum time step used in the numerical solution routine was

established in 1 hour. The calibration procedure was based on direct experimental determination as well as on curve fitting of experimental data monitored. The effective diffusion coefficient of the pollutant (D) and the effective specific surface area (a_s) were the set of parameters estimated by curve fitting during the model calibration step. To start with the calibration procedure, initial guesses were assigned to the estimated parameters. Predicted Cr(III) liquid concentration by the model was compared with the experimentally measured data (C^*) and the deviations between both were used to obtain updates for the estimated parameters. Parameter values were sought to minimize the objective function (OF) given in equation 12.

$$OF = \sqrt{\sum_{i=1}^{N} \left[C\,(D, a_s) - C^* \right]^2} \qquad (12)$$

Where N is the number of measurements realized and C* is the measured concentration of the solute (mg L^{-1}).

The parameter estimation was performed using a MATLAB algorithm based on a multidimensional unconstrained nonlinear minimization (Nelder-Mead) algorithm. This is a direct search method that does not use numerical or analytical gradients. Model calibration and validation of the present work was checked by performing a statistical analysis based on a paired t-Student's test at the 5% level of significance.

Results and Discussion

Effect of the Initial Chromium Concentration

In order to test the leonardite potential as sorbent for industrial applications, columns filled with leonardite were tested in continuous mode by passing Cr(III) solutions at different concentrations. A total of 6 tests were performed in order to assess the initial

concentration effect on the column performance. Figure 1 shows the corresponding breakthrough curves for 6 different initial concentrations. All columns were run for the same period of time (3000 min). As expected, the effect of the initial chromium concentration on breakthrough curves is critical. Breakthrough time, defined as the time required to reach a specific breakthrough outlet concentration, decreases with increasing metal concentration. This means that higher metal loading rates generates lower adsorption zone lengths. In addition, the initial slope of the breakthrough curves became steeper when the initial concentration was increased, showing that the reaction zone advances faster at high load conditions. Almost 36 hours were necessary to obtain a measurable chromium outlet concentration for the lowest initial concentrations, demonstrating quite good behavior of the leonardite in continuous operation.

Application of the Analytical Models

In order to depict clearly the model predictions for the analytical equations (equations 2-3 and 5-8) only 4 inlet concentrations are shown. Model predictions for the BDSM, Thomas and Yoon and Nelson are summarized in figure 2. In addition model parameters are listed in table 2.

The Borhart-Adams (figure 2a) approach gave fairly good predictions for the experimental behavior (excepting for the highest initial Cr(III) concentration). However, despite the equation was originally derived to describe the initial section of the breakthrough curve, it gave acceptable results for the whole data sets. This might be attributed to the fact that BDSM models imply the use of two parameters to be adjusted, reducing the number of degrees of freedom and, thus, giving a more accurate fitting. From the adjustment procedure by nonlinear regression, the sorption capacity of the sorbent (N_0) is obtained. The values calculated (between 80-130 mg L^{-1}) are, as

285 expected, clearly lower than those obtained in previous batch tests (data not shown).
286 This also suggests that BDSM model must be regarded as an empirical mathematical
287 expression (or a particular solution to a general problem) capable to fit a set of
288 experimental data. The assumption considered by this model, that the rate of adsorption
289 is controlled by the surface reaction between the sorbate and the remaining active sites,
290 could explain the experimental behavior observed. Further conclusions or information
291 derived for design purposes should be under suspect.
292 The worst predictions were obtained for the Thomas model approach (figure 2b). The
293 main assumptions of this model (no mass transfer limitation and second order kinetics)
294 seem to fail in predicting the continuous adsorption of Cr(III) in leonardite. The results
295 suggest some sort of mass transfer resistance as dominating step for the column
296 performance. The use of only one single parameter to fit the equation is another
297 drawback of the approach. The squared sums of errors (ERRSQ) for this model were by
298 far the largest computed among all model approaches.
299 Similar results (in terms of ERRSQ) to the BDST were obtained for the Yoon and
300 Nelson model. Despite this is an empirical equation based on probabilistic aspects of the
301 sorption process, the time to 50% sorbate breakthrough ($t_{0.5}$) are quite realistic as it is
302 shown in figure 2c and table 1. The only important deviation is observed for the lowest
303 inlet concentration (20 mg L^{-1}), although the model predictions are acceptable even in
304 this case as shown by the low ERRSQ value.
305 Figure 3a shows the predictions of the Clark model. Apparently only slight differences
306 from BDSM and Yoon and Nelson can be observed. The Clark model assumes some
307 sort of mass transfer resistance (external or internal) and Freundlich equilibrium
308 isotherm behavior. Even though the model contains information regarding to mass
309 transfer resistance issues, this phenomenon is lumped to operational parameters.

310 Therefore, it is (again) difficult to draw relevant information from the model itself.
311 From table 2, it is not possible to establish a relationship between the r parameter and
312 the initial concentration, although the Clark model parameter is related to the migration
313 velocity of the concentration front in the bed. Again, the use of a two-parameter
314 approach results in lower ERRSQ values.
315 Similar to the BDSM model, the Wolborska analytical expression was developed for
316 predicting the first part of the breakthrough curve. In this sense, figure 3b shows that
317 effectively the model predictions fail to fit the experimental data except for the lowest
318 concentration. For a better model fitting, only the first part of the experimental
319 breakthrough curve was considered in order to obtain parameters in table 2. N_0 values,
320 despite higher than those predicted by the BDST model, are still much lower than
321 experimental batch values. An increase of N_0 values when increasing the initial
322 concentration was expected but not observed. Again, this places some serious doubts
323 about the usefulness of the analytical solutions approach.
324 As already stated, the Dose-Response model is based on mathematical issues instead of
325 mechanistic information. From the information plotted in figure 3c and listed in table 3,
326 it is clear that model predictions are fairly good or, at least, as good as BDST, Clark and
327 Yoon and Nelson models. This can be also concluded by checking the ERRSUM values
328 listed in table 3. However, the values of the chromium concentration in the solid phase
329 (q_0) (table 3) are 100 times lower than those measured in batch experiments.
330 From the discussion above it is clear that analytical solutions models are a simple and
331 useful technique for data fitting, but they hardly supply any information regarding the
332 mechanisms involved in the chromium removal. In addition, from design purpose point
333 of view, the suitability of such approaches is also under suspect.
334

335 ***Application of the New Modeling Approach***

336 Analytical model solutions must be regarded as simple approaches to the real column
337 behavior. Even though their use implies a fast and easy procedure, the information that
338 can be derived from the equations used in the previous section is hardly useful for
339 scaling-up and real applications design purposes. In this sense, a balance between
340 mathematical complexity and model reliability is needed in order to obtain useful tools
341 capable to come up with design-related information.

342 The model developed, which fulfills the above stated requirements, is a simple and
343 powerful tool able to describe most of the mass-transfer related processes. It is based on
344 a mass balance along the column considering plug flow and the mass transfer from the
345 liquid to the sorbent as a function of the concentration gradient and the equilibrium
346 isotherm. The main objective of the model setup is to characterize the kinetic sorption
347 of the continuous (column) system by adjusting the minimum number of parameters.
348 The value of coefficient diffusion denotes the relative rate of transfer through the
349 material (i.e. sorption rate) and makes possible to quantitatively compare the behavior
350 of different materials by means of a parameter with physical information in contrast to
351 classical empirical models.

352 Figure 4 shows Cr(III) concentrations at the column outlet jointly with the model
353 predictions after the calibration step for an inlet concentration of 100 mg L^{-1}. The
354 effective diffusion coefficient for Cr(III) in leonardite obtained in the procedure is
355 $2.92 \cdot 10^{-6}$ m^2 h^{-1} and the effective area is $2.9 \cdot 10^5$ m^2 m^{-3}. This value corresponds only to
356 an 8% of the total area of the material ($3.73 \cdot 10^6$ m^2 m^{-3}). As it is also shown in Figure 4,
357 the statistical analysis based on a paired t-Student's test at 5% of significance shows a
358 good agreement between results predicted by the model with the optimized parameters
359 and experimental data.

Once the kinetic parameters were calibrated for the specific experiment shown above, model validation was performed by comparing the simulation results to experimental data in the same set of experiments shown in Figure 1. The comparative results obtained in the validation step are shown in Figure 5. A satisfactory global agreement is observed between experimental data and model predictions, especially for 20, 40 and 150 mg L^{-1} . In the case of 75 mg L^{-1}, the concentrations predicted are slightly different than those registered experimentally. However, it should be noted that the breakthrough curve at this concentration is less consistent with the experimental behavior of the rest of concentrations and an early material saturation was expected.

It is worth mentioning that the new model approach, unlike analytical models, has been calibrated and validated with different experimental data showing a good agreement in both scenarios by means of the same set of parameters. Thus, a good description of the process has been checked for a wide range of cases.

Comparing the agreement between experimental and model predictions achieved by analytical models and those obtained by the new model approach, the latter is able to describe more satisfactory the behavior experimentally observed, according to the ERRSQ values. As shown in Table 1 and 2, the average ERRSQ for each model is between a minimum value of 0.0334 for the Response-Dose and a maximum of 1.3262 for the Yoon and Nelson. In the case of the new model approach the average ERRSQ is 0.0254 which means an improvement of 24% with respect to the best fitting previously achieved with the analytical models.

Conclusion

A comparison between classical analytical solutions and a simple unsteady-state mass balances-based approach for breakthrough curves prediction was presented. Analytical solutions showed good capabilities for experimental data fitting despite hardly any conclusion could be derived from their adjustment. In addition, extrapolation of their predictions must be avoided. The numerical approach described offered a good balance between mathematical easiness and rigorous description of the main phenomena occurring in the gas-solid mass transfer process. The model presented herein allowed obtaining a powerful predictive tool together with relevant process parameter values (effective area and effective diffusion coefficient).

Acknowledgements

The Spanish government (MEC) provided financial support through the project CICYT CTQ2008-06842-C02-02.

References

[1] Fendorf, S.E. Surface Reactions of Chromium in soils and waters. Geoderma. **1995**, *67*, 55-67.

[2] Esmaeili, A.; Mesdaghi, A.; Vazirinejad, R. Chromium (III) removal and recovery from tannery wastewater by precipitation processes. Am. J. Appl. Sci. **2005**, *10*, 1471-1473.

[3] Vasudevan, S.; Lakshmi, J.; Vanathi, R. Electrochemical Coagulation for Chromium Removal: Process optimization, Kinetics, Isotherms and Sludge Characterization. Clean-Soil Air Water. **2010**, *38*, 9-16.

409 [4] Liguori, B.; Cassese, A.; Colella, C. Safe immobilization of Cr (III) in heat-treated
410 zeolite tuff compacts. J. Hazard. Mater. **2006**, *137*, 1206-10.

411 [5] Mousavi, S. A.; Mirbagheri, S. A.; Mohammadi, T. Using Reverse Osmosis
412 Membrane for Chromium Removal from Aqueous Solution. World Academy of
413 Science, Engineering and Technology. **2009,** *57*, 348-352.

414 [6] Lao, C.; Zeledon, Z.; Gamisans, X. Solé, M. Sorption of Cd(II) and Pb(II) from
415 aqueous solutions by a low-rank coal (leonardite). Sep. Purif. Technol. **2005**, *45*, 79-85.

416 [7] Zeledón, Z.; Lao, C. Sole, M. Nickel and copper removal from aqueous solution by
417 an immature coal (leonardite): effect of pH, contact time and water hardness. J. Chem.
418 Technol. Biot. **2005,** *80*, 649-656.

419 [8] Zeledón**,** Z., Lao, C., de las Heras, F. X. C. Sole, M. Removal of PAHs from water
420 using an immature coal (leonardite). Chemosphere. **2005**, *67*, 505–512.

421 [9] Mohan, D.; Pittman C. U. Jr. Activated carbons and low cost adsorbents for
422 remediation of tri- and hexavalent chromium from water. J. Hazard. Mater. **2006**, *137*,
423 762-811.

424 [10] Bohart, G.; Adams, E. Q. Some aspects of the behavior of charcoal with respect to
425 chlorine. J. Am. Chem. Soc. **1920**, *42*, 523-544.

426 [11] Srivastava, V.C.; Prasad, B.; Mishra, I.M.; Mall, I.D.; Swamy, M.M. Prediction of
427 breakthrough curves for sorptive removal of phenol by bagasse fly ash packed bed. Ind.
428 Eng. Chem. Res. **2009**, *47*, 1603-1613.

429 [12] Unuabonah, E.I.; Olu-Owolabi, B.I.; Fasuyi, E.I.; Adebowale, K.O. Modeling of
430 fixed-bed column studies for the adsorption of cadmium onto novel polymer-clay
431 composite adsorbent. J. Hazard. Mater. **2010**, *179*, 415-423.

432 [13] Thomas, H. C. Heterogeneous ion exchange in a flowing system. J. Am. Chem.
433 Soc. **1944**, *66*, 1664-1666.

434 [14] Yoon, Y. H.; Nelson, J. H. Application of gas adsorption kinetics. I. A theoretical
435 model for respirator cartridge service time. Am. Ind. Hyg. Assoc. J. **1984**, *45*, 509-516.

436 [15] Clark, R. M. Evaluating the cost and performance of field-scale granular activated
437 carbon systems. Environ. Sci. Technol. **1987**, *21*, 573-580.
438 [16] Wolborska, A. Adsorption on activated carbon of p-nitrophenol from aqueous
439 solution. Water Res. **1989**, *23*, 85-91.
440 [17] Yan, G.Y.; Viraraghavan, T.; Chem, M. A new model for heavy metal removal in a
441 biosorption column, Adsorpt. Sci. Technol. **2001**, *19*, 25–43.
442 [18] Cutlip, M.B.; Shacham, M. *Problem solving in chemical and biochemical*
443 *engineering with POLYMATH, EXCEL and MATLAB*. Prentice Hall, New York, 2008.
444 [19] Lao, C.; Solé, M.; Gamisans, X.; Valderrama, C.; Dorado A.D. Characterization of
445 Chromium (III) removal from aqueous solutions by an immature coal (Leonardite).
446 Towards a better understanding of the phenomena involved. Clean Technol. Envir.
447 **2012**, (In press).
448

FIGURES CAPTIONS

Figure 1. Breakthrough curves for the adsorption of Cr(III) onto leonardite in a fixed bed column used for process modeling.

Figure 2. Model predictions (lines) for the BDSM (a), Thomas (b) and Yoon and Nelson (c) models.

Figure 3. Model predictions (lines) for the Clark (a), Wolborska (b) and Dose-Response (c) models.

Figure 4. Experimental outlet concentration and numerical approach model predictions in the calibration step corresponding to a Cr(III) inlet concentration of 100 mg L^{-1}.

Figure 5. Experimental outlet concentration and model predictions in the validation procedure corresponding to a Cr(III) inlet concentration of 20, 40, 75 and 150 mg L^{-1}

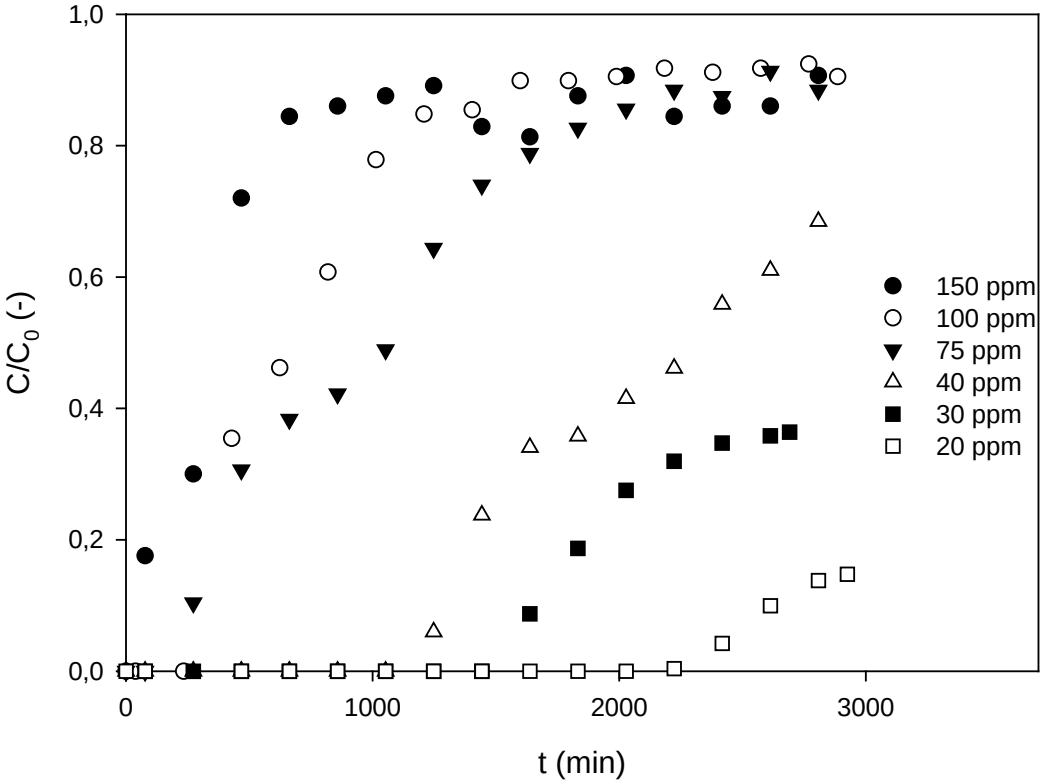
1,0
0,8
0,6
0,4
0,2
0,0
C/C0 (-)
0
1000
2000
3000
t (min)
150 ppm
100 ppm
75 ppm
40 ppm
30 ppm
20 ppm

Fig. 1

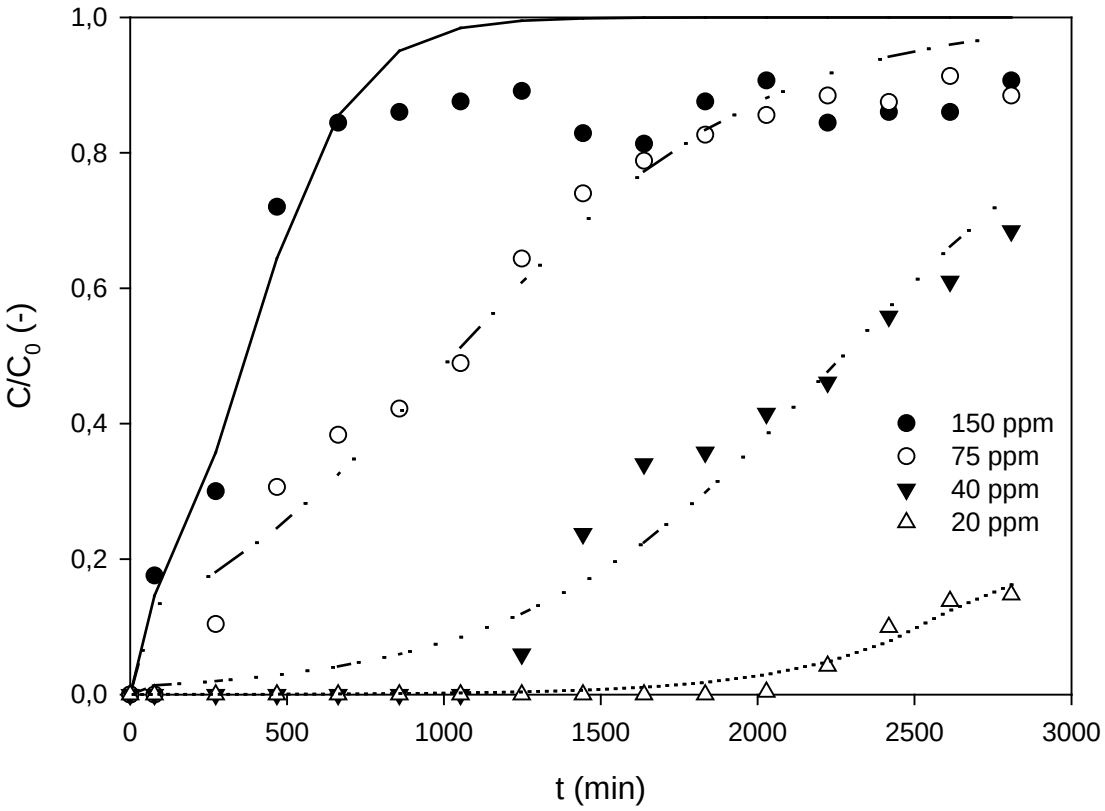
1,0
0,8
0,6
0,4
0,2
0,0
C/C0 (-)
0
500
1000
1500
2000
2500
3000
t (min)
150 ppm
75 ppm
40 ppm
20 ppm

Fig. 2a

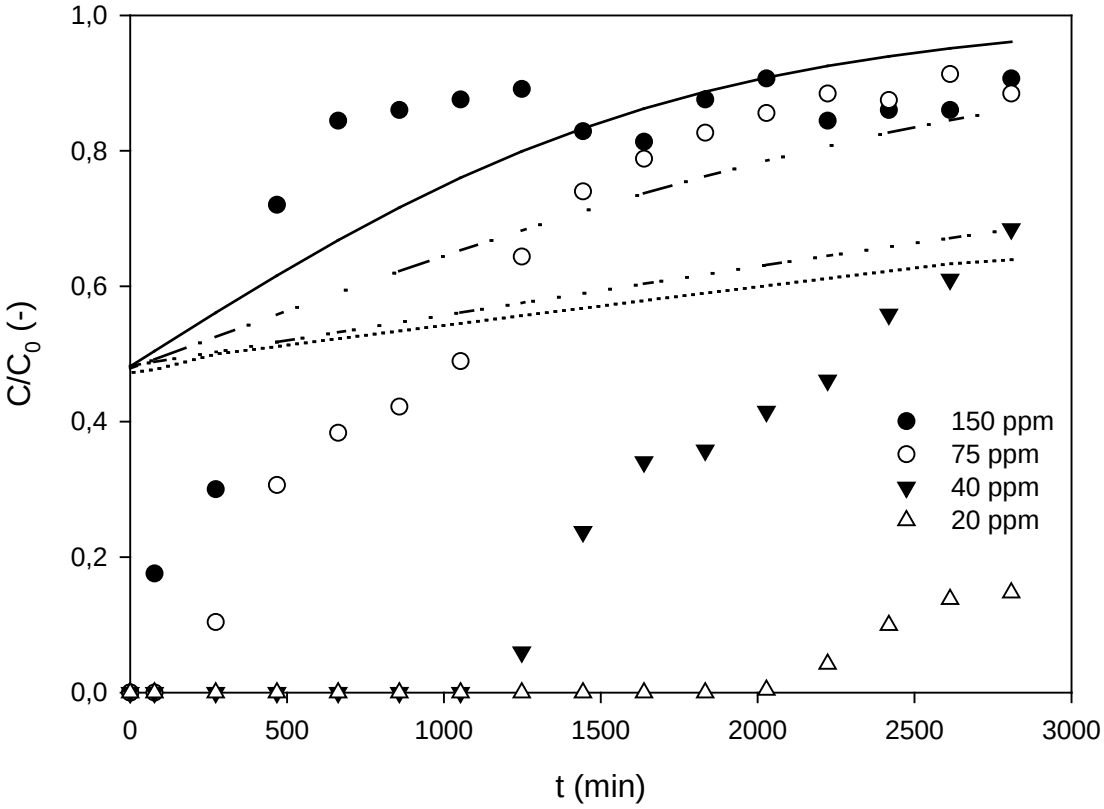
1,0
0,8
0,6
0,4
0,2
0,0
C/C0 (-)
0
500
1000
1500
2000
2500
3000
t (min)
150 ppm
75 ppm
40 ppm
20 ppm

Fig.2b

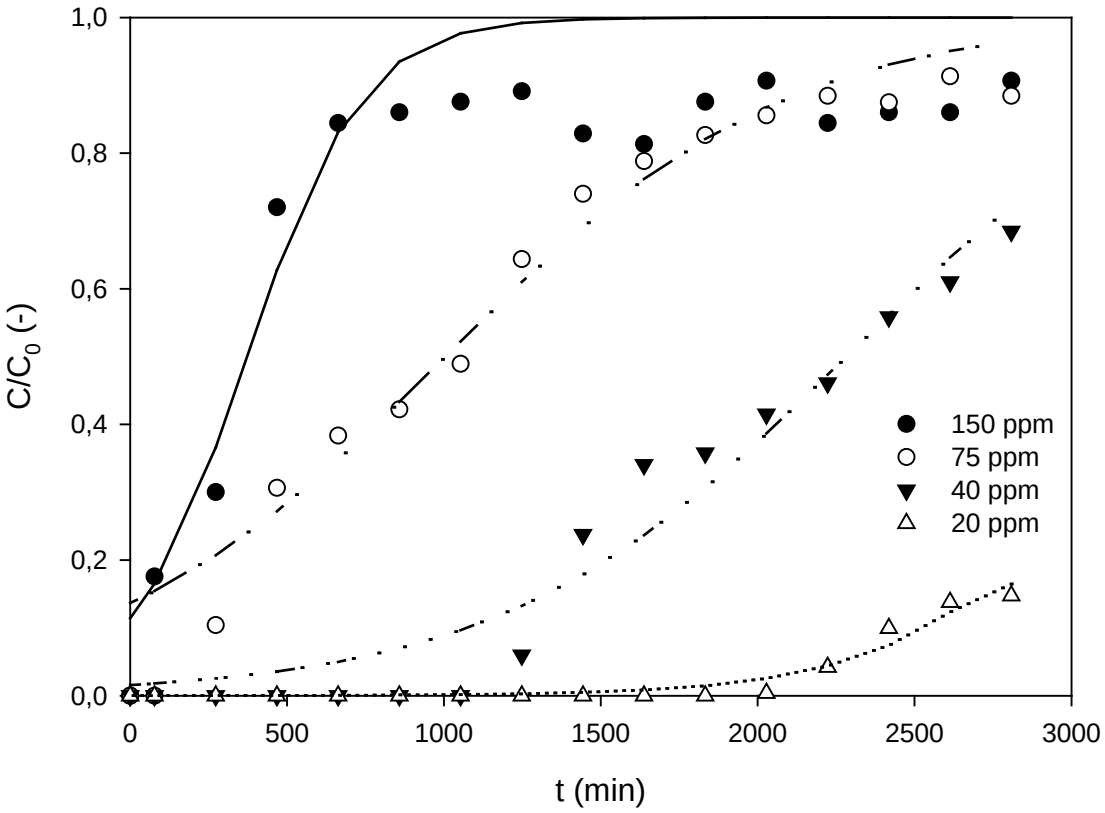
1,0
0,8
0,6
0,4
0,2
0,0
C/C0 (-)
0
500
1000
1500
2000
2500
3000
t (min)
150 ppm
75 ppm
40 ppm
20 ppm

Fig.2c

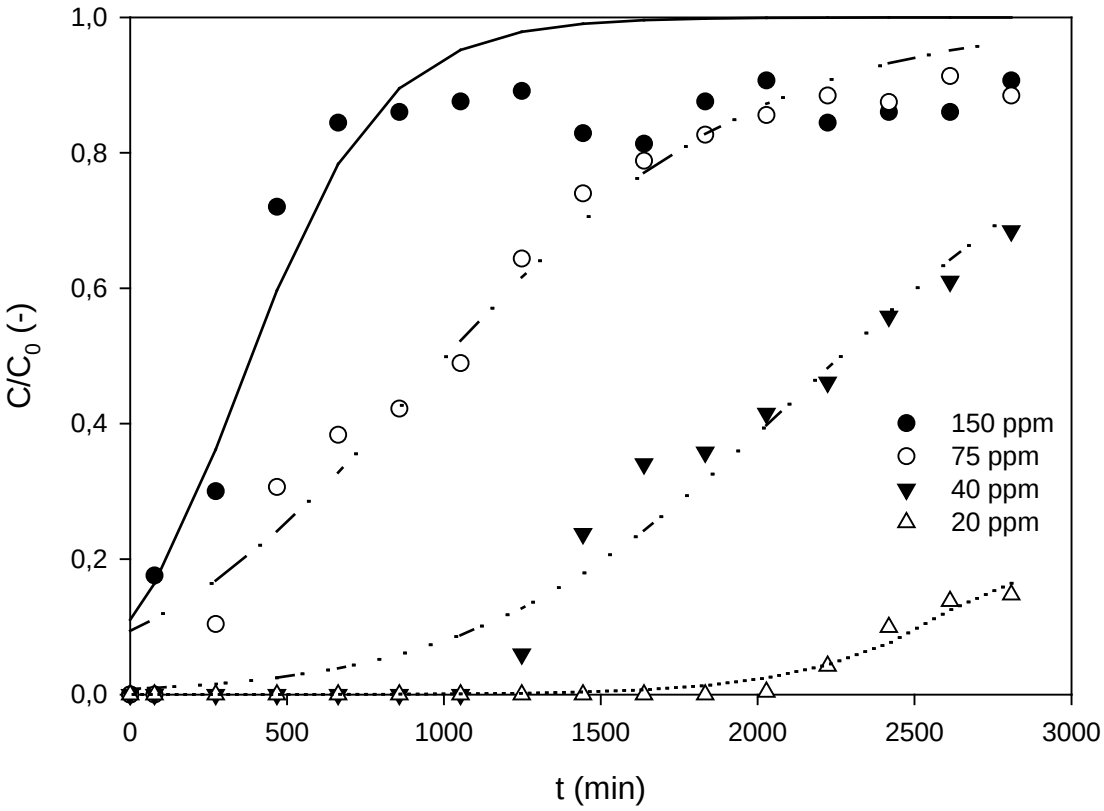
1,0
0,8
0,6
0,4
0,2
0,0
C/C0 (-)
0
500
1000
1500
2000
2500
3000
t (min)
150 ppm
75 ppm
40 ppm
20 ppm

Fig. 3a

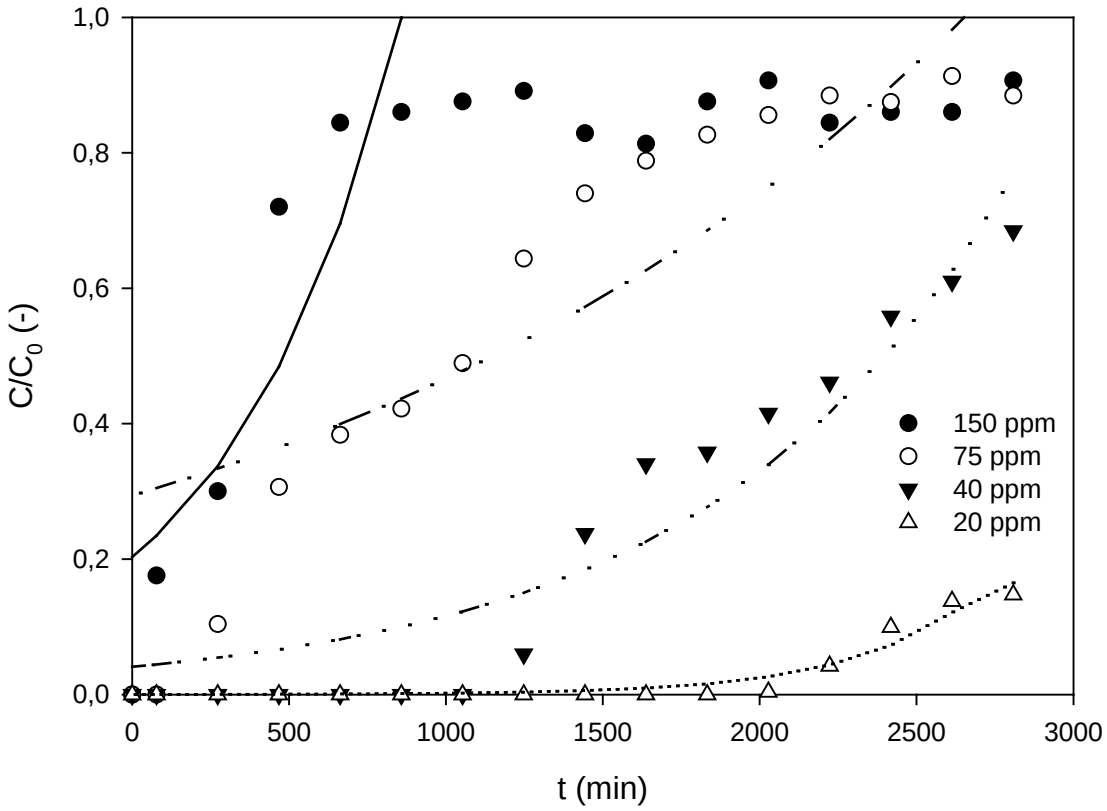
1,0
0,8
0,6
0,4
0,2
0,0
C/C0 (-)
0
500
1000
1500
2000
2500
3000
t (min)
150 ppm
75 ppm
40 ppm
20 ppm

Fig.3b

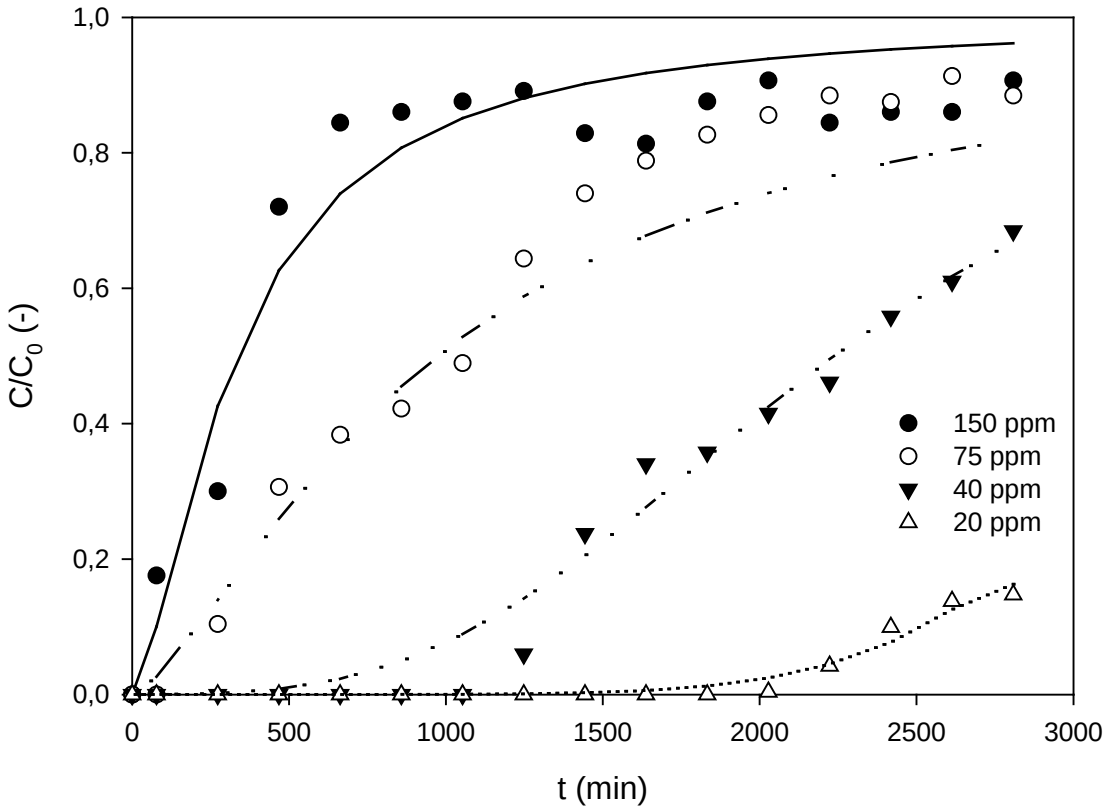
1,0
0,8
0,6
0,4
0,2
0,0
C/C0 (-)
0
500
1000
1500
2000
2500
3000
t (min)
150 ppm
75 ppm
40 ppm
20 ppm

Fig. 3c

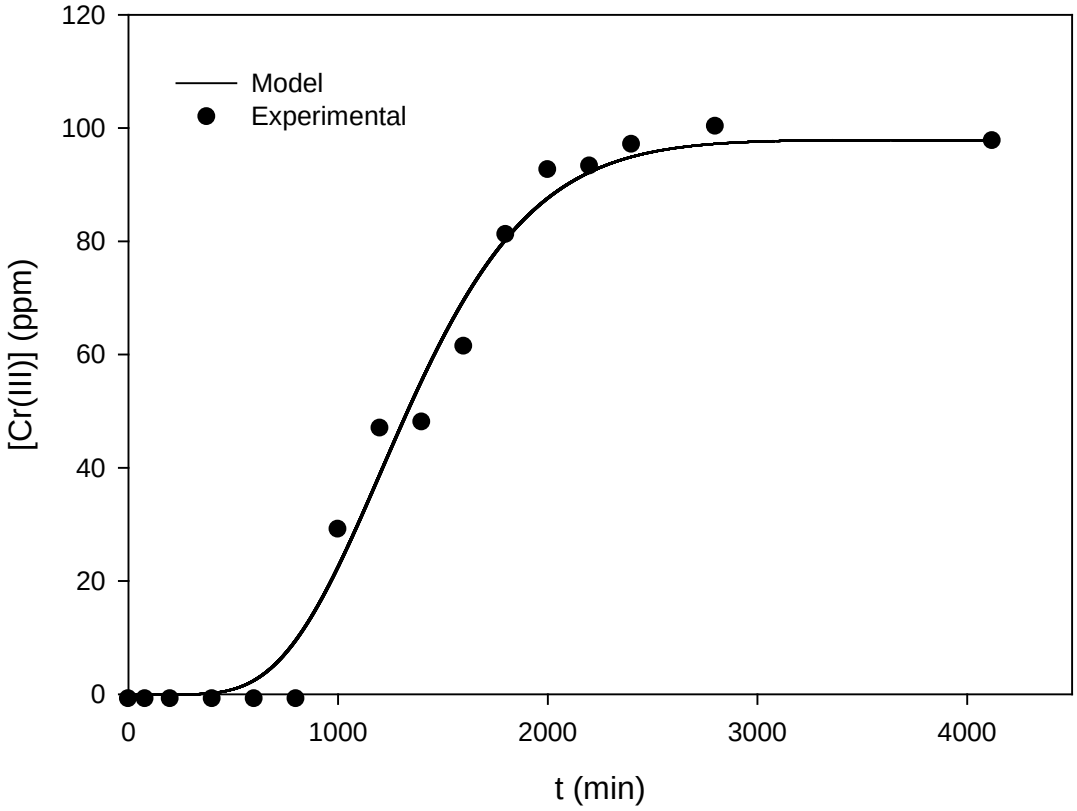
Model
Experimental
[Cr(III)] (ppm)
t (min)
0
20
40
60
80
100
120
0
1000
2000
3000
4000

Fig. 4

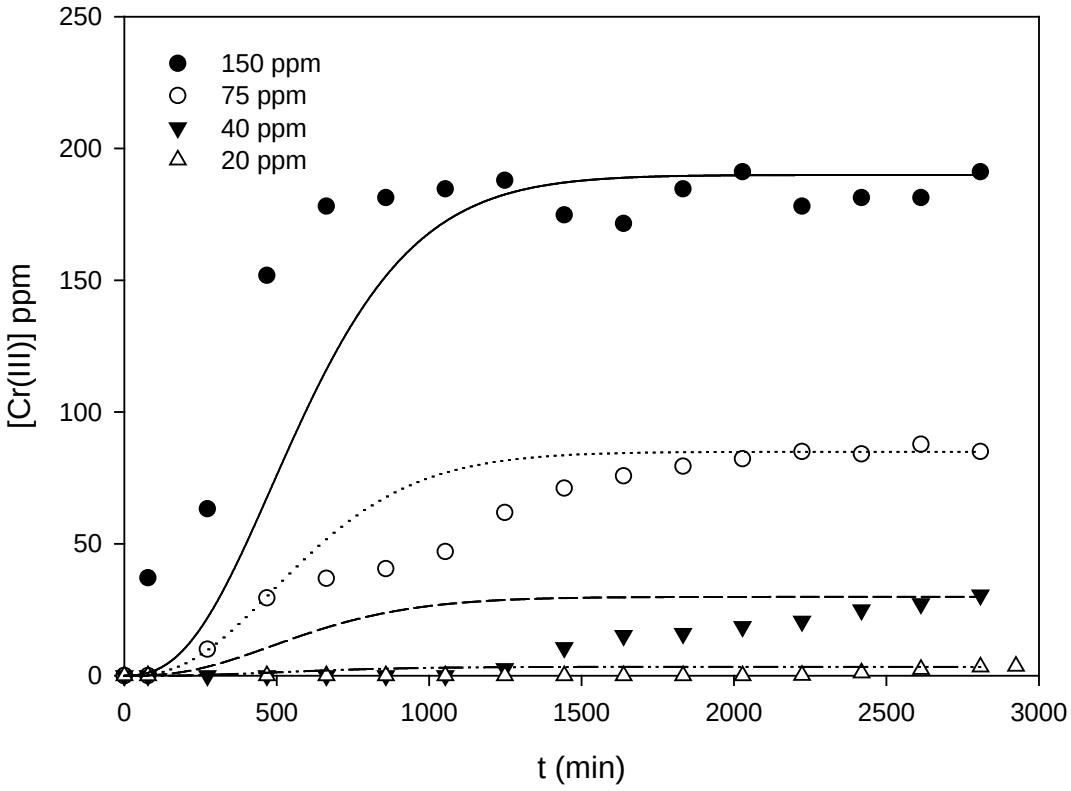
250
200
150
100
50
0
[Cr(III)] ppm
150 ppm
75 ppm
40 ppm
20 ppm
0
500
1000
1500
2000
2500
3000
t (min)

Fig.5

Table 1. Chemical composition and physical properties of leonardite (SEPHU®) used in this study.

Property	Value
Humic acids (%)	79.0
C (%)	55.2
H (%)	3.4
N (%)	0.8
O (%)	38.1
S (%)	2.4
BET area ($m^2\ g^{-1}$)	19.9
Moisture (%)	30.0
Density ($g\ mL^{-1}$)	1.67
Cationic exchange capacity ($meq\ g^{-1}$)	2.87
Single bond COOH groups ($meq\ g^{-1}$)	3.12
Single bond OH groups ($meq\ g^{-1}$)	2.07

Table 2. Model parameters and ERRSQ values for the BDST, Thomas and Yoon and Nelson models.

	BDST			**Thomas**		**Yoon and Nelson**		
C_0 (mg L^{-1})	N_0 (mg L^{-1})	K (L min^{-1} mg^{-1})	ERRSQ (-)	k_T (L min^{-1} mg^{-1})	ERRSQ (-)	k_{YN} (min^{-1})	$t_{0.5}$ (min)	ERRSQ (-)
20	99.33	0.00793	0.0015	0.000700	0.972	0.00288	3488.38	0.0019
40	127.53	0.00293	0.1420	0.000450	0.617	0.00182	2281.88	0.0445
75	114.28	0.00160	0.0498	0.000546	2.275	0.00184	1004.65	0.0299
150	81.24	0.00242	0.0241	0.000466	1.441	0.00549	372.95	0.2440

606

607 **Table 3.** Model parameters and ERRSQ values for the Clark, Wolborska and Dose-Response models.

608

	Clark			**Wolborska**			**Response-Dose**		
C_0 (mg L^{-1})	A (-)	r (min^{-1})	ERRSQ (-)	N_0 (mg L^{-1})	B (min^{-1})	ERRSQ (-)	a (-)	q_0 (mg g^{-1})	ERRSQ (-)
20	591.67	0.119	0.0016	101.20	0.795	0.0022	7.47	0.200	0,0015
40	14.42	0.090	0.0355	171.53	0.269	0.0888	3.09	0.246	0,0134
75	2.81	0.105	0.0397	278.66	0.103	0.2951	1.43	0.201	0,0055
150	2.48	0.255	0.2380	180.40	0.134	0.1503	1.51	0.137	0,1134

609